Supplemental Figure 1

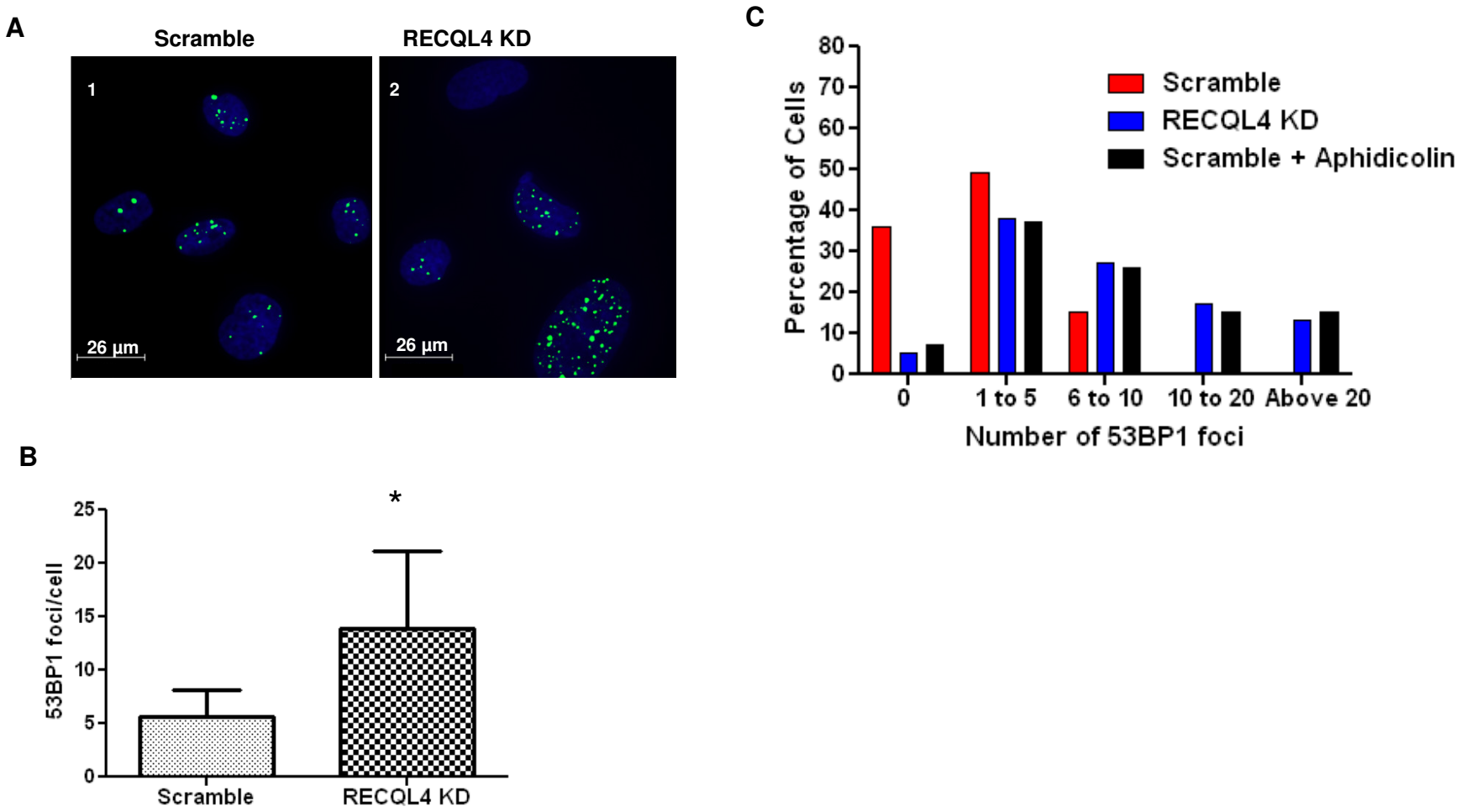

(A) Representative microscopic images showing 53BP1 foci (green) in Scramble and RECQL4 depleted (RECQL4 KD) U2OS cells. DAPI (blue) is used for nuclear staining. **(B)** Quantitative analysis showing the average 53BP1 foci per cell in Scramble and RECQL4 KD U2OS cells. Error bars represent standard deviations from three independent experiments. The difference was statistically significant ($p<0.05$, $n=30$). **(C)** Histograms showing the frequency distribution of 53BP1 foci in Scramble, RECQL4 KD and aphidicolin treated Scramble U2OS cells ($n = 40$).

Supplemental Figure 2

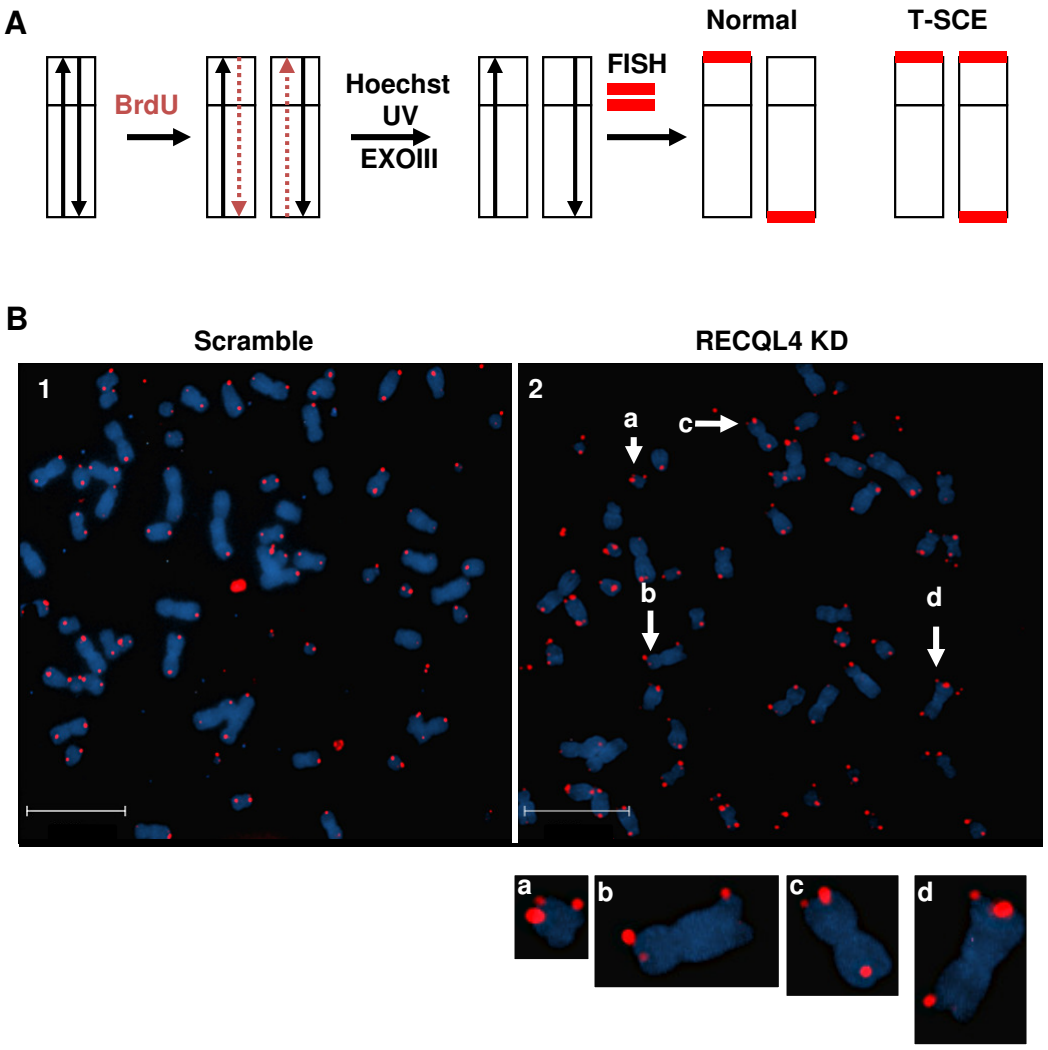

(A) Schematic of COFISH. **(B)** Microscopic images showing representative metaphase spreads from Scramble and RECQL4 KD U2OS cells. Some telomere sister chromatid exchanges are marked by arrows and shown as individual images.

Supplemental Figure 3

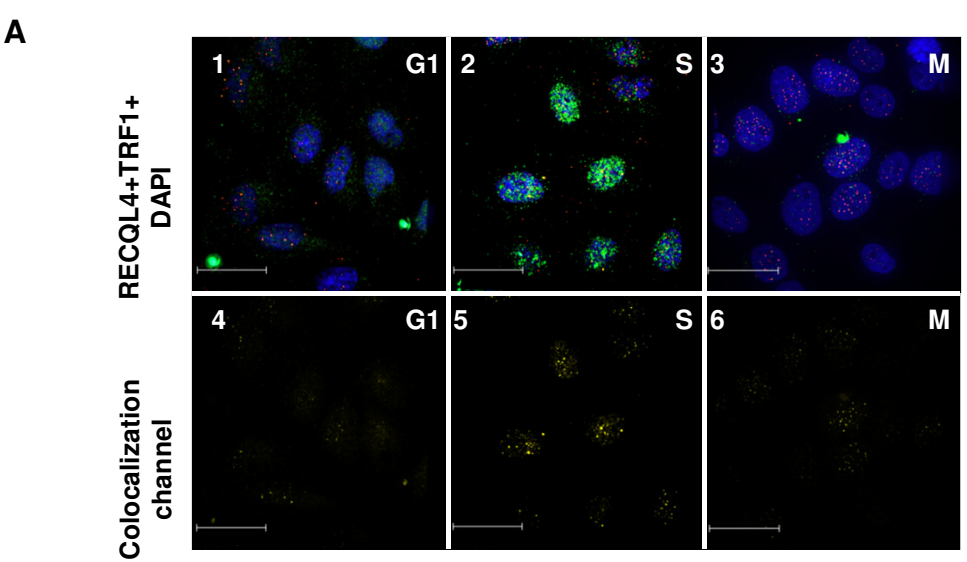

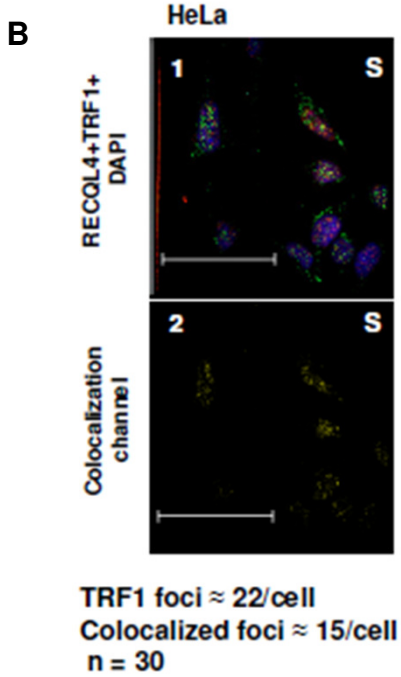

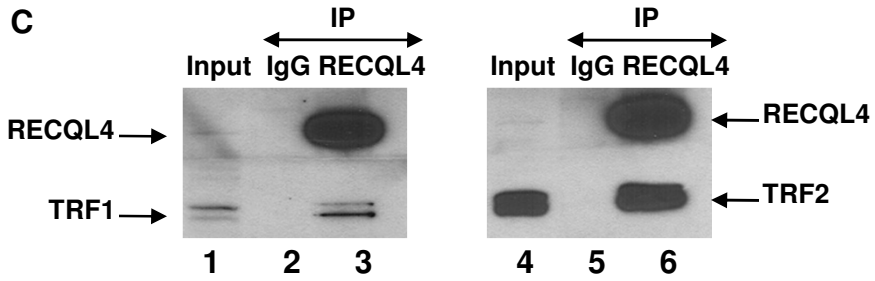

(A) Confocal microscopic images of representative U2OS cells showing colocalization of RECQL4 (green) and TRF1 (red) during G1, S and M phase. DAPI (blue) is used a nuclear marker. Colocalized foci are shown as yellow dots (Lanes 4-6). **(B)** Confocal microscopic images of representative HeLa cells showing colocalization of RECQL4 (green) and TRF1 (red) during S phase. DAPI (blue) is used a nuclear marker. Colocalized foci are shown as yellow dots (Lane 2). Numbers of TRF1 foci and colocalized foci per cell are also mentioned (n = 30). **(C)** *In vivo* co-immunoprecipitation (IP) in U2OS cell of TRF1 (Lanes 1-3) and TRF2 (Lanes 4-6) by RECQL4. Lane 1 and 4 represent input, showing the bands corresponding to RECQL4, TRF1 and TRF2. Lanes 2 and 5 represent IP with IgG controls and lanes 3 and 6 represent the IP with antibodies specific to RECQL4. Bands corresponding to anti-RECQL4, anti-TRF1 and anti-TRF2 antibodies are marked.

Supplemental Figure 4

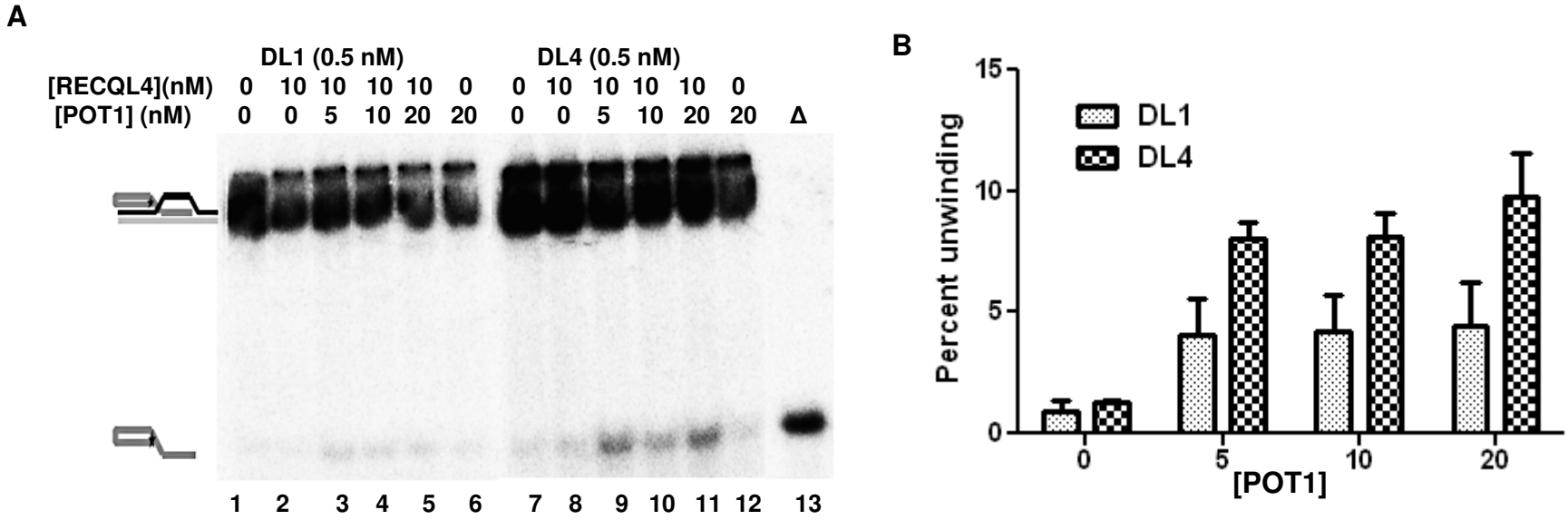

(A) Autoradiogram showing the unwinding activity of RECQL4 (10 nM) on 0.5 nM DL1 (lanes 1-5) and DL4 (lanes 7-11) in presence of 0, 5, 10 and 20 nM GST-POT1. Δ (Lane 13) represents heat denatured DL4. The destabilizing activity of 20 nM GST-POT1 alone on DL1 and DL4 is shown in lane 6 and lane 12, respectively.**(B)** Histograms showing the unwinding activity of RECQL4 (10 nM) on 0.5 nM DL1 and DL4 in presence of 0, 5, 10 and 20 nM GST-POT1.The signals corresponding to the single stranded DNA generated by the destabilizing effect of POT1 was subtracted from each value. Error bars represent standard deviation from the average of three independent experiments.

Supplemental figure 5

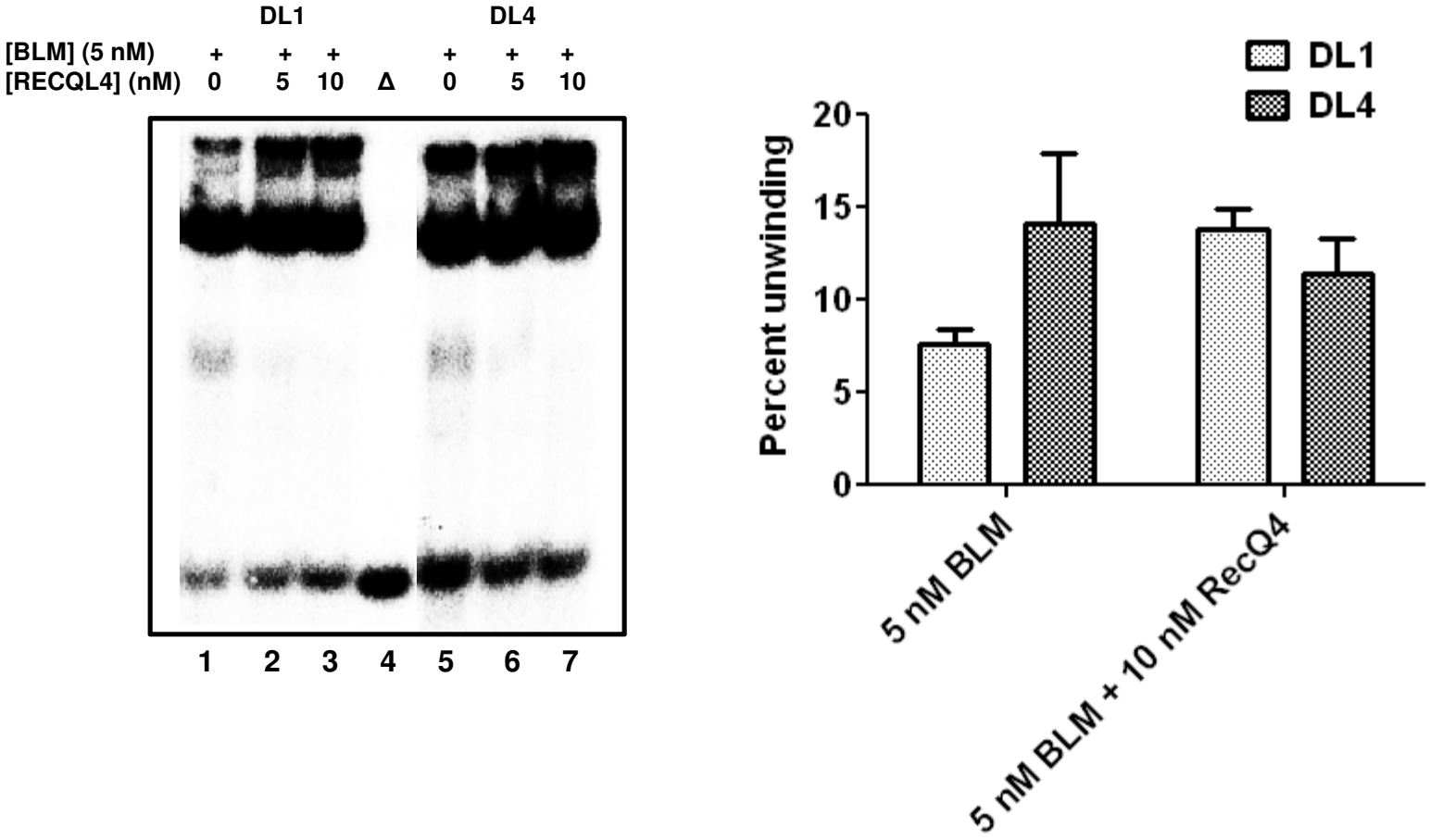

(A) Autoradiogram showing the effect of RECQL4 (5 and 10 nM) on the helicase activity of 5 nM BLM on 0.5 nM DL1 (lanes 1-3) and DL4 (lanes 5-7). Lane 4 represents heat denatured DL4.**(B)** Histograms showing the unwinding activity of BLM (5 nM) on 0.5 nM DL1 and DL4 in presence of 10 nM Error bars represent standard deviation from the average of three independent experiments.